Electronic structure, magnetic properties, and exchange splitting of gadolinium intermetallics

Brian Ensign[1], Renu Choudhary[1], Huseyin Ucar[2], and Durga Paudyal[1]

[1]Critical Materials Institute, Ames Laboratory, Iowa State University, Ames, IA-50011

[2]California State Polytechnic University, Pomona, CA 91768

We report here the electronic structure calculations of the magnetic moment, magneto-crystalline anisotropy energy (MAE), and density of states (DOS) of Gd-metal, $GdAl_2$, $GdAl_3$, $GdCo_2$, $GdCo_3$, and $GdCo_5$. From the DOS, the exchange splitting energy is derived to map ferrimagnetic to paramagnetic phase transition (Curie temperature, T_C). The employed theoretical method here is based on advanced density functional theory, specifically the linearized augmented plane wave method (LAPW) within the local spin density approximation (LSDA), including spin-orbit coupling (SOC) and Hubbard model parameter (U). DOS analysis of both Gd-Al and Gd-Co systems reveals a strong correlation between exchange splitting energy and T_C. The Gd-Co system exhibits an enormous exchange splitting energy among Co-3*d* electrons, vastly overwhelming the vanishing Gd 5*d* exchange splitting. These findings suggest that exchange splitting of Co-3*d* electrons plays a key role in the ground state magnetism and magnetic transition temperatures in these materials.

1. Introduction

Currently, the most popular magnetic materials contain significant concentrations of rare earth (RE) elements that provide strong magneto-crystalline anisotropy while transition metals (TM) impart large saturation magnetization at high temperatures. For instance, the current "champion" magnet, $Nd_2Fe_{14}B$, constitutes as much as 62% of the world market for permanent magnets [1]. $SmCo_5$, while less common, offers some advantages, most notably a higher Curie temperature than $Nd_2Fe_{14}B$ as well as the largest known uniaxial MAE of 17.2 MJ/m^3 [2,3]. However, the erratic and often volatile supply of these RE elements can make them cost-prohibitive [1].

In the ongoing search for improved magnetic performance and reduced criticality of RE supply chains, it is essential to understand and predict the magnetic properties of new materials. This study utilizes a computational method known as advanced density functional theory to calculate *ab initio* the magnetic properties of elemental Gd, $GdAl_2$, $GdAl_3$, $GdCo_2$, $GdCo_3$, and $GdCo_5$. $GdAl_5$ is not included, as it does not form [4].

Despite its high intrinsic spin moment, gadolinium tends to make a poor basis for permanent magnets. This is because the half-filled 4*f* states have spherically symmetric charge density, and thus exhibit virtually no magnetic anisotropy. However, this does make Gd a useful component for investigations into magnetocaloric refrigeration which depends on the rapid reversal of

magnetization, thus making a large hysteresis undesirable [5,6]. The intermetallic $GdCo_2$, on the other hand, is investigated for its potential to be used in magneto-optical applications due to sizeable Faraday rotations achievable in these compounds [7]. Much as Gd, $GdCo_5$ is explored with *ab initio* techniques because of its symmetric 4*f* shell electronic state giving rise to a net-zero orbital magnetization and a vanishing crystal electric fields (CEF). Virtually zero CEF in this compound makes it an attractive test-bed for elucidating the role of RE-TM exchange interactions. In addition, its magnetization increases with temperature due to Gd moments disordering more rapidly than Co in the lattice. The opposing Gd and Co moments also give rise to a compensation temperature at which the net magnetization is zero. These experimental observations were reproduced with the use of first principles calculations [8,9]. In one particular study, Nguyen et. al. used an on-site Coulomb *U* and exchange *J* corrections even at the 3*d* electrons of cobalt to better reproduce the experimental data on $GdCo_5$ compounds [10]. As far as the magnetic anisotropy of this ferrimagnetic compound is concerned, first principles calculations fail to predict its value and exhibit wrong temperature dependence because of the presence of a number of magnetic sublattices. Despite these challenges, Patrick et. al. were able to predict correct anisotropy values by calculating the temperature dependent magnetization versus field curves within the context of disordered local moment formalism [11]. Inspired by the earlier research, this study analyzes the fundamental electron behavior of these compounds, with the aim of better understanding RE-transition metal magnetic properties, especially T_C. This study focuses primarily on Gd-Co compounds, as the high T_C of cobalt (1394 K) lends itself naturally to investigations into raising the T_C of RE-based magnets through alloying [10]. Despite the non-magnetic nature of aluminum, the properties of $GdAl_2$ are also presented here to give useful insight as to the nature of the magnetic interactions in the Gd sublattice.

In order to understand the electronic structure of these intermetallics, it is essential that we describe the crystal structure of each and point out the common features that are present [12]. In many RE-TM systems of interest, AB_2 type Laves phases are observed with the larger RE atom as the A element and smaller TM as B. $GdCo_2$ has the cubic Laves phase with Gd forming a diamond sublattice and Co tetrahedra occupying the empty tetrahedral sites of the structure as shown in Figs. 1 (a) and (d) which show both the unit cell of this C15 structure along with the projection of all atoms from a cell in to the (010) plane respectively. $GdCo_3$, on the other hand, has a rhombohedral unit cell with the space group, $R\bar{3}m$. This structure is similar to the hexagonal Laves phase $MgNi_2$ mainly because while $MgNi_2$ has a six-fold rotation symmetry, $GdCo_3$ has three-fold roto-inversion symmetry as indicated by the $\bar{3}$ in the space group. We show this structure in a hexagonal prismatic representation as in Fig. 1 (b) along with the projection of atoms on the (001) plane as in Fig 1 (e). As for the $GdCo_5$, its structure is that of a $CaCu_5$ as the prototype (P6/mmm, No.191). This structure can be described as alternating layers of hexagonal nets formed by the TM atoms (2c) with the RE sitting at the center of the net, and planes of TM atoms (3g) arranged in a Kagome network as shown in Figs. 1 (c) and (f). Here, it is important to realize that the hexagonal structure of $GdCo_5$ is related to the $MgNi_2$ Laves phase as $GdCo_3$, and because all these intermetallics are somehow related to the well-known Laves phases, the

connected tetrahedrons either by sharing vertices or faces is a common feature of these structures.

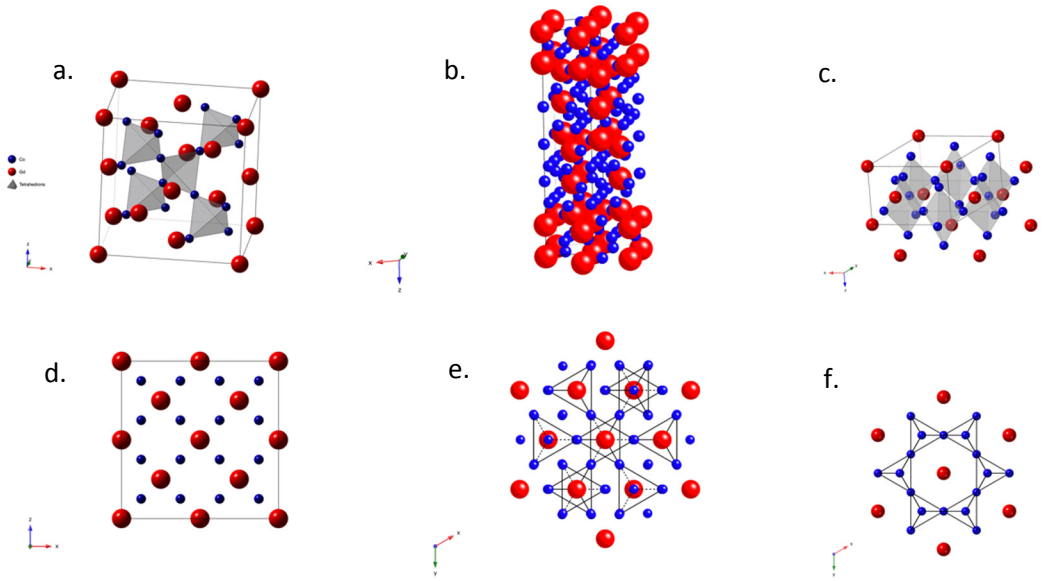

Figure 1. Crystal structure depictions of the atoms in their respective unit cells: (a) $GdCo_2$ Laves phase (b) $GdCo_3$ and (c) $GdCo_5$ and the projections of all atoms into the (010) planes for the $GdCo_2$ (d), into the (001) planes for the (e) $GdCo_3$ and (f) $GdCo_5$.

2. Computational Method

The calculations were carried out with the WIEN2k code, a full potential, linearized augmented plane wave DFT method [13]. The k-space integrations have been performed at least with 15 × 15 × 17 Brillouin zone mesh which was sufficient for the convergence of total energies (10^{-6} Ryd.), charges, and magnetic moments. For RCo_5 systems, the higher values of plane-wave cut-off ($RK_{max.}$ = 9.0 and $G_{max.}$ = 14) are required [14].

This study employs the local spin-density approximation (LSDA), which essentially treats conduction electrons as a gas of non-interacting particles and then approximates the exchange-correlation interactions based solely on the electron density at each point in space. Some difficulty arises in using this approximation for gadolinium because of the seven unpaired 4*f* electrons. These electrons are not entirely localized, and an adequate description of their itinerancy and correlation has been elusive [15, 16]. A more recent investigation strongly suggests that LSDA is adequate if the 4*f* electrons are treated as part of the valence band and a correction is made for on-site correlation [17]. An effective Hubbard parameter (*U-J*) of 6 eV was used in

these calculations. Additionally, for each compound except $GdCo_3$, the energy was calculated with the moment aligned along the *a*-axis and *c*-axis, the expected anisotropic axes for cubic and hexagonal systems. For the rhombohedral $GdCo_3$, the moment was aligned along the [100] and [111] directions.

3. Results and Discussions

3.1. Magnetic Moment

Table 1 shows the calculated ground-state magnetic moments alongside the experimental values and previous theory work for comparison. The orbital moment of Gd is near zero as expected, but with 7 unpaired 4*f* electrons, the spin magnetic moment is relatively large compared to other RE elements. In Gd-Co compounds, Co's spin moment aligns anti-parallel to Gd's spin moment, showing the ferrimagnetic ordering in Gd-Co compounds [18] whereas, in Gd-Al compounds, moment on aluminum is negligible (~ -0.01 μ_B), showing ferromagnetic ordering in all Gd-Al compounds. Therefore, all Gd-Co compounds are ferrimagnets, whereas all Gd-Al compounds are ferromagnets.

Table 1: Calculated and experimental magnetic moments of Gd-intermetallics.

	Magnetic Moment (μ_B per f.u.)					
	Gd	$GdAl_2$	$GdAl_3$	$GdCo_2$	$GdCo_3$	$GdCo_5$
$\mu_{Tot,}$ *present*	7.69	7.40	7.09	5.17	3.62	0.55
$\mu_{Tot,}$ *exp*	7.12[19]	7.2[20], 7.1[21]	8.29[22]	4.89[23]	3.30[24], 2.85[25]	1.42[26]
$\mu_{Tot,}$ *theory*	7.77 (FM)* [27] 7.43 (PM)+ [28]	7.48 (FM)° [29] 7.34 (PM)‡ [29]		4.36¥ [30]	3.01 (FM)§ [31] 3.6 (PM)§ [31]	1.29◊ [32] 0.62◊ [9] 2.59● [10]

** Local Spin Density Approximation (LSDA) with Hubbard parameter (+U) and Korringa-Kohn-Rostocker (KKR) formulation*
+ Linear Muffin Tin Orbital (LMTO) in the Atomic Sphere Approximation (ASA)
° LSDA+LMTO+ASA
‡ LSDA + Disordered Lattice Model (DLM) with Coherent Potential Approximation (CPA)
¥ Stochastic Quenching (SQ)
§ LSDA + U + Tight-binding LMTO + ASA
◊ DLM + KKR + CPA
● Generalize Gradient Approximation (GGA) + U

Theoretically calculated magnetic moments agree well with the experimental results except for $GdAl_3$ and $GdCo_5$. The experimental value of the magnetic moment for $GdAl_3$ is higher than our theoretically calculated moment. This discrepancy could be because of the magnetic frustration with competing for exchange interactions of $GdAl_3$ [33, 34]

Similarly, $GdCo_5$ exhibits an experimental magnetic moment higher than our theory prediction. This may be attributable to the non-collinear nature of magnetic configuration in cobalt atoms, whereas the calculations assumed a collinear configuration. Previous work by Radwaǹski [35] has demonstrated a theoretical model for describing the conditions of non-collinearity for $GdCo_5$.

Due in large part to the spherically symmetric 4*f* charge density in Gd atoms, each material in this study is predicted to have small magneto-crystalline anisotropy energy. Precise calculations of such small MAE are beyond the scope of this study. We thus present here no details on the MAE calculations. However, it is worth mentioning that MAE for each of these compounds were predicted to be on the order of a few μeV both theoretically [27, 36] and experimentally [37, 38, 39].

3.2. Density of States

The density of states near the Fermi level is of particular interest, as this region describes behavior of the conduction electrons. Figs. 2a-f show the DOS of the Gd-5*d*, Co-3*d* and Al-3*p* electrons. For each intermetallic, the nature of exchange splitting – an energetic displacement across the Fermi level of the up-spin and corresponding down-spin peaks along the x-axis – is different. First, because the conduction electrons such as Al-3*p* states are free, there is very little exchange splitting between majority and minority spin states with a population density that is nearly equal as shown in Figs. 2b and 2c. On the contrary, narrow *d*-bands do show sizeable exchange splitting owing to the fact that the energy savings due to exchange interactions are higher than the kinetic energy cost to putting all these electrons in higher k-states. This is formulated as the Stoner criterion for ferromagnetism:

$$I(E_F)N(E_F) > 1,$$

where $I(E_F)$ is the Stoner parameter, and $N(E_F)$ is the DOS at the Fermi level. This indicates that magnetism is present in materials with strong exchange interactions and large DOS at the Fermi level [40].

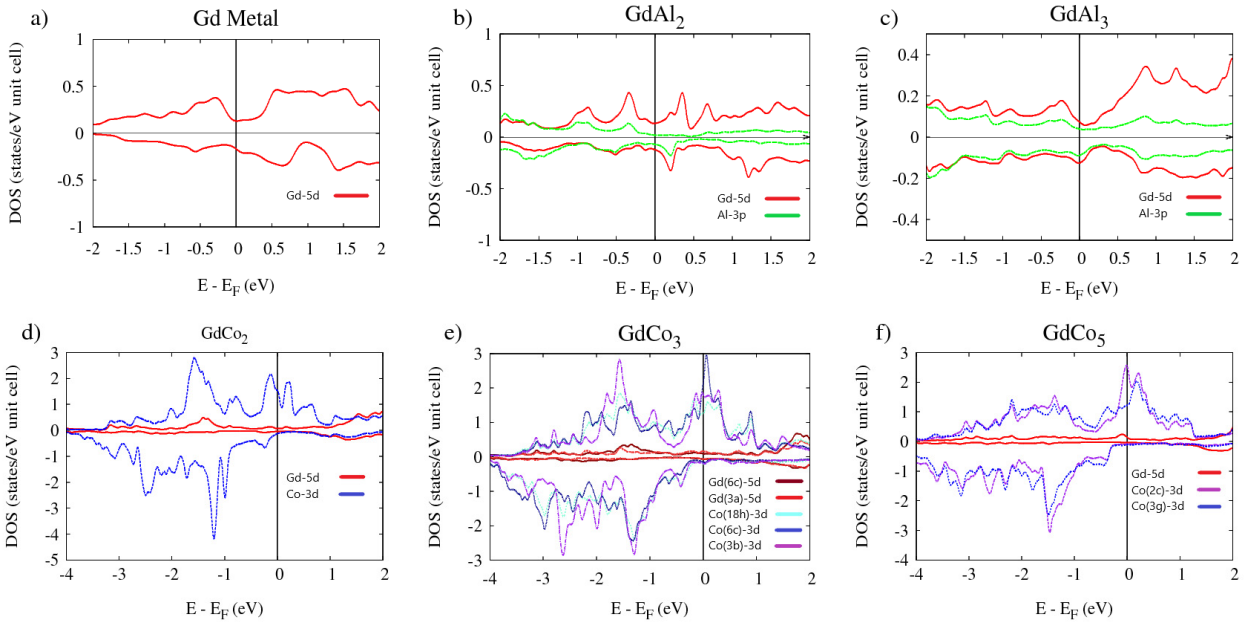

Figure 2: DOS of Gd (a), $GdAl_2$ (b), $GdAl_3$ (c), $GdCo_2$ (d), $GdCo_3$ (e), and $GdCo_5$ (f)

Since the difference between the spin DOS integrals over an energy range yields the magnetic moment contribution of the electrons in that range, exchange splitting in the conduction band can lead to a net magnetic moment as one spin direction becomes preferred below the Fermi level. This is the case in the Gd-Co class of compounds, as the net band moment opposes the large localized Gd-4*f* moments, thus contributing to ferrimagnetism. This coupling between the RE-TM atoms is mediated by the 5*d* electrons of Gd as evidenced by the hybridization between 5*d* electrons of Gd and 3*d* electrons of Co near the Fermi level for each intermetallic in Figs. 2d-f. As the temperature increases and the up-spin states above the Fermi level become occupied by these itinerant electrons due to reduced exchange splitting, we would expect a decrease in the overall magnetic moment.

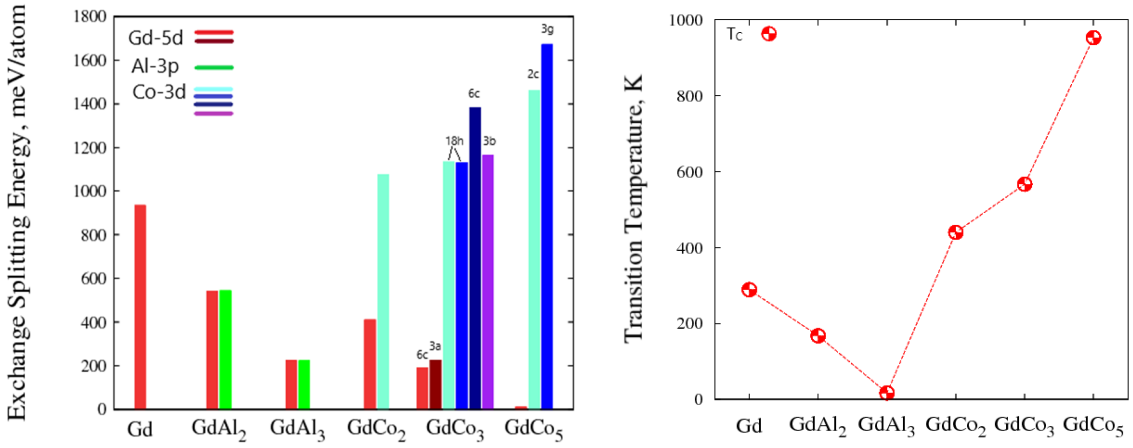

Figure 3: Exchange splitting energies of distinct atom sites, alongside corresponding T_C[27, 37, 41, 42, 43, 44].

Figure 3 summarizes the exchange splitting energies of the crystallographically distinct atoms in each compound, plotted along with the corresponding T_C obtained experimentally [27, 37, 41, 42, 43, 44]. In the Gd-Al system, the addition of aluminum evidently decreases the exchange interactions between Gd-5*d* electrons, which corresponds to a decrease in T_C. Since $GdAl_3$ exhibits less exchange splitting than $GdAl_2$, it can also be inferred that the splitting of Al-3*p* is a product of polarization by Gd-5*d*.

In the Gd-Co system, the addition of cobalt also decreases the exchange splitting in Gd-5*d*. Nevertheless, T_C continues to increase along with the Co-3*d* exchange splitting energy. This suggests that the exchange interactions in Co-3*d* are a far more significant driver of magnetic transition temperatures than the interactions among the Gd-5*d* electrons. This is consistent with earlier reports on RE-TM magnets in which the consensus is that that high-temperature magnetism is predominantly governed by 3*d* electrons of TMs while low-temperature magnetism is dominated by *f* electrons [18,45]. If we compare our exchange splitting energy data with the experimental values of Curie temperature, we can notice that exchange splitting energy is directly proportional to the Curie temperature. It may be possible to reasonably predict transition temperatures for any RE-TM composition based on exchange splitting energies. Thus, exchange splitting energy – while certainly not the only factor – is a useful guide for estimating T_C. To get a more quantitative understanding of T_C, mean-field approximations can be used in which the inter-site exchange couplings, $J_{i,j}$, calculated by Liechtenstein's method [41] are mapped onto a classical Heisenberg Hamiltonian given by:

$$\mathcal{H} = -\sum_{i,j} J_{i,j}\vec{e}_i\vec{e}_j$$

Where, $J_{i,j}$ is the exchange constant and $\vec{e}_i$ is a unit vector designating the direction of the local spin moment.

In this work, we have calculated Curie temperature only for Gd-metal by taking energy difference of ferromagnetic and antiferromagnetic configurations. The the energy difference, $J = E_{AFM} - E_{FM}$, is 30.935 meV per Gd-atom. Our estimated Curie temperature for Gd metal is ~ 239 K, calculated using relation $T_C = 2J/3k_B$, where k_B is Boltzmann constant. The calculated Curie temperature is of the same order as the experimental value. Understanding the coupling between the exchange splitting energy and the Curie temperature will be our future work.

4. Conclusions

We have calculated the magnetic moments of Gd, $GdAl_2$, $GdAl_3$, $GdCo_2$, $GdCo_3$, and $GdCo_5$ using *LSDA* with spin-orbit coupling (*SOC*) and Hubbard parameter (*U*). We plot the density of states of their itinerant electrons. In both the Gd-Al and Gd-Co systems, we find that increased Al or Co concentration decreases the exchange interactions of Gd-5*d* electrons. The decreased 5*d* exchange splitting with increased Al composition reduces the 4*f*-5*d* exchange, thereby reducing

the indirect 4*f*-4*f* interaction and resulting in decreased Curie temperature. On the other hand, the increased 3*d* exchange splitting results in the increased Co-3*d* – Co-3*d* interactions, which intimately allows for increased Curie temperature with higher content of Co. In the Gd-Al system, Al-3*p* exchange splitting seems to be largely a result of hybridization with Gd-5*d*—a polarization effect which LSDA likely exaggerates. In the Gd-Co system, Gd-5d exchange splitting is reduced; however, a radical increase in Co-Co exchange interactions dominate which drives up T_C. This demonstrates the utility of DOS analysis in understanding magnetic behavior and offers the possibility of employing exchange splitting energy as a predictor of magnetic transition temperatures in RE-TM systems. Further work will include finding a relation between the exchange splitting energy and the Curie temperature and also understanding Nd-based intermetallic systems, as Nd offers unusual and intriguing magnetic anisotropy and ordering in the ground state. [46]

Acknowledgments

This research is supported by the Critical Materials Institute, an Energy Innovation Hub funded by the US Department of Energy. Work at the Ames Laboratory was supported by the U.S. Department of Energy Office of Science, Science Undergraduate Laboratory Internship (SULI) program under its contract with Iowa State University, Contract No. DE-AC02-07CH11358. Brian Ensign is grateful to the DOE for the assistantship and opportunity to participate in the SULI program. A special thanks to Ed Moxley for his technical support on this project, and Mitchell Henderson for his beneficial theoretical and computational discussions.

References

[1] O. Gutfleisch, M. A. Willard, E. Brück, C. H. Chen, S. G. Sankar, and J. P. Liu, Adv. Mat. **23-7**, 841 (2011).

[2] A. Landa, P.Söderlind, D. Parker, D. Åberg, V. Lordi, A. Perron, P.E.A. Turchi, R.K. Chouhan, D. Paudyal, T.A. Lograsso, J. Alloys. Comp. **765**, 659 (2018).

[3] J.M.D. Coey, IEEE Trans. Magn. **47**, 4671 (2011).

[4] I. Shidlovsky and W. E. Wallace, Journal of Solid-State Chem. **2**, 193 (1970).

[5] G.Lorusso, E. Natividad, M. Evangelisti, and O. Roubeau, Mater. Horiz, **6**, 144 (2019).

[6] A. Waske, M. Gruner, T. Gottschall, and O. Gutfleisch, MRS Bulletin **43 (4)**, 269 (2018).

[7] S. J. Lee, R. J. Lange, P. C. Canfield, B. N. Harmon, and D. W. Lynch, Phys. Rev. B **61,** 9669 (2000).

[8] C. E. Patrick, S. Kumar, G. Balakrishnan, R. S. Edwards, M. R. Lees, E. Mendive-Tapia, L. Petit, and J. B. Staunton, Phys. Rev. Materials **1**, 024411 (2017).

[9] A. L. Tedstone, C. E. Patrick, S. Kumar, R. S. Edwards, M. R. Lees, G. Balakrishnan, and J. B. Staunton, Phys. Rev. Materials **3**, 034409 (2019).

[10] M. C. Nguyen, Y. Yao, C.-Z. Wang, K.-M. Ho and W. P. Antropov, J. Condens. Matter Phys., **30** 195801, (2018).

[11] C. E. Patrick, S. Kumar, G. Balakrishnan, R. S. Edwards, M. R. Lees, L. Petit, and J. B. Staunton, Phys. Rev. Lett. **120**, 097202 (2018)

[12] Crystallographic information from: SpringerMaterials, Pierre Villars (Chief Editor), PAULING FILE in: Inorganic Solid Phases, Springer, Heidelberg (ed.), https://materials.springer.com

[13] P. Blaha, K. Schwarz, G.K.H. Madsen, D. Kvasnicka, J. Luitz, *WIEN2k: An Augmented Plane Waves Plus Local Orbitals Program for Calculating Crystal Properties*, Vienna University of Technology, Austria (2001).

[14] O. Eriksson, R. Ahuja, A. Ormeci, J. Trygg, O. Hjortstam, P. Söderlind, B. Johansson, and J.M. Wills, Phys. Rev. B **52**, 4420 (1995).

[15] J. Sticht, J. Kübler, Solid State Comm. **53**, 529 (1985).

[16] D.J. Singh, Phys. Rev. B **44**, 1751 (1991).

[17] Ph. Kurz, G. Bihlmayer, S. Blügel, J. Phys. Condens. Matter **14**, 6353 (2002).

[18] R. Skomski, J. Appl. Phys. **83**, 6724 (1998).

[19] J. F. Elliott, S. Legvold and F. H. Spedding, Phys. Rev., 91, 28-30 (1953).

[20] E. W. Lee, J. F. D. Montenegro, J. Mag. Mag. Mater. 22, 282-290 (1981).

[21] W. M. Swift, W. E. Wallace, J. Phys. Chem. Solids 29, 2053 (1968).

[22] K. H. J. Buschow, and J. F. Z. Fast, Phys. Chem. **50**, 51 (1966).

[23] K. Fujiwara, K Ichinose, and A. Tsujimara, J. Phys. Soc. Jpn. **56**, 2149 (1987).

[24] Q.A. Li, G. F. Zhou,N. Tang,F. R. De Boer,K. H. J. Buschow, J. Alloys Compd. 201 (1993) 185-189.

[25] S. K. Malik, E. B. Boltich , W. E. Wallace, Solid State Commun. 37, 329-333 (1981).

[26] T. Okamoto, H. Fujii, C. Inoue, and E. Tatsumoto, J. Phys. Soc. Jpn. **34**, 835 (1973).

[27] L. Oroszlány, A. Deák, E. Simon, S. Khmelevskyi, and L. Szunyogh, Pys. Rev. Lett. **115**, 096402 (2015).

[28] W. M. Temmerman, P. A. Sterne, J. Phys.: Condens. Matter **2**, 5529-5538 (1990).

[29] I. Turek, J. Rusz, and M. Divis, J. Magn. Magn. Mater. **290–291**, 357 (2005).

[30] R. Lizarraga, Phys. Rev. B **94**, 174201 (2016).

[31] R. Tetean, E. Burzo, and L. Chioncel, J. Alloys. Comp. **430**, 19-21 (2007).

[32] C. E. Patrick, S. Kumar, G. Balakrishnan, R. S. Edwards, M. R. Lees, E. Mendive-Tapia, L. Petit, and J. B. Staunton, Phys. Rev. Mat. **1**, 024411 (2017).

[33] B R Coles, S Oseroff, and Z Fisk, J. Phys. F: Met. Phys. **17**, L169-LI71 (1987).

[34] N. N. Delyagin et al., Solid State Communications **150**, 1231–1233 (2010).

[35] R.J. Radwańnski, Physica **142B**, 57 (1986).

[36] M. Colarieti-Tosti, S. I. Simak, R. Ahuja, L. Nordström, O. Eriksson, M. S. S. Brooks, J. Mag. Mag. Mat. **272-276**, Supplement, E201 (2004).

[37] T. Katayama and T. Shibata, J. Mag. Mag. Mat. **23**, 173 (1981).

[38] D. Gignoux, F. Givord, and R. Lemaire, J. Phys. Rev. B **12**, 3878 (1975).

[39] N. Kaplan, E. Dormann, K.H.D. Buschow, and D. Le-Bendaum, Phys. Rev. B **7**, 40 (1973).

[40] R. C. O'Handley, *Modern Magnetic Materials: Principles and Applications*, Wiley, (1999).

[41] A. I. Liechtenstein, M. Katsnelson, V. Antropov, and V. Gubanov, J. Magn. Magn. Mat. **67**, 65, (1987).

[42] Kittel, Charles, *Introduction to Solid State Physics* (6th ed.). John Wiley and Sons. (1986).

[43] M. Kwiecien, G. Chełkowska, K. Rabijasz, J. Alloys. Comp. **423**, 55 (2006).

[44] G. Chelkowska, J. Magn. Magn. Mat. **127**, L37 (1993).

[45] M. Matsumoto, R. Banerjee, and J. B. Staunton, Phys. Rev. B **90**, 054421 (2014).

[46] J. W. Cable, R. M. Moon, W. C. Koehler, and E. O. Wollan, Phys. Rev. Lett. **12**, 553 (1964).